Taylor & Francis
Taylor & Francis Group

REPORT

⌢ OPEN ACCESS   Check for updates

Kinetic analysis of ternary and binary binding modes of the bispecific antibody emicizumab

Stefanie Mak, Agnes Marszal, Nena Matscheko, and Ulrich Rant [ID]

Dynamic Biosensors GmbH, Munich, Germany

ABSTRACT

The binding properties of bispecific antibodies (bsAb) are crucial for their function, especially when two antigens are targeted on the same cell surface. Dynamic interactions between each of the antibody's arms and its cognate target cause the formation and decay of a biologically functional ternary complex. How association and dissociation processes work cooperatively, and how they influence the avidity of the ternary complex, is still poorly understood. Here, we present a biosensor assay for the simultaneous measurement of the binding kinetics of the therapeutic bsAb emicizumab (Hemlibra®) and its two targets, the blood coagulation factors IX and X (FIX, FX). We describe an automated workflow to characterize binary and ternary-binding modes, utilizing a Y-shaped DNA nanostructure to immobilize the antigens on a sensor and to emulate conditions on a cell or platelet surface by presenting the antigens with optimal accessibility for the bsAb flown over the sensor as analyte. We find that emicizumab binds FX much stronger than FIX (K_d = 0.05 µM vs. 5 µM, $t_{1/2}$ = 20 s vs. 1 s) with profound consequences on the avidity of the ternary complex, which is dominated by FX's binding properties and a hand-off mechanism from FX to FIX. Moreover, formation and decay of the ternary complex depend on the bsAb concentration during the association phase. Emicizumab's in-vivo mode of action and the catalytic activation of FX can be rationalized from the analyzed binding kinetics. The assay and workflow are well suited for the screening of bispecific binders in drug discovery and provide valuable new kinetic information.

Abbreviations: bsAb: bispecific antibody; FVIII/FIX/FX: coagulation factors VIII/IX/X; SPR: surface plasmon resonance; k_{on}: association rate constant; k_{off}: dissociation rate constant; K_D: equilibrium dissociation constant; $t_{1/2}$: dissociation half-life

Introduction

Bispecific antibodies (bsAbs) are engineered binders, designed to target two chemically distinct epitopes simultaneously.[1] This unique binding mode can be used to induce previously unattainable mechanisms of action, which have great potential for many therapeutic applications in oncology, autoimmune diseases, chronic inflammatory diseases, bleeding disorders, and even infectious diseases like COVID-19.[2] Bispecific formats have become highly prominent in current drug development pipelines, as can be seen, for example, for monoclonal antibodies in late-stage clinical studies with a regulatory submission anticipated in 2021–2022 for cancer indications, half of which are in fact bispecific.[3] While some bsAbs stimulate an immune response by connecting immune cells to cancer cells, like the US Food and Drug Administration (FDA)-approved bispecific T cell engagers blinatumomab (Blincyto®, Amgen, FDA approval 2014) or tebentafusp (Kimmtrak®, Amgen, FDA approval 2022), others are designed to bind two different antigens on the surface of the same cell.[4,5] In the latter case, dual targeting serves either to identify a target cell with superior selectivity, or to induce proximity of two antigens on a cell to modulate signaling or enzymatic activity. Recently approved

therapeutics based on the dual-targeting-on-same-cell approach include amivantamab (Rebrevant®, Janssen, FDA approval 2022) and emicizumab (Hemlibra®, Chugai/Roche, FDA approval 2017). Amivantamab binds to two tumor-associated antigens, EGFR and c-MET, which facilitates hetero-dimerization and results in the downmodulation of oncogenic signaling. Emicizumab, which resulted from seminal work of Kitazawa et al.,[6] was the second bsAb approved by the FDA and paved the way for the use of bispecifics beyond T cell engagers. It is used to treat the bleeding disorder hemophilia A by mimicking the activity the missing coagulation factor VIII (FVIII). It does so by forming a ternary complex with the membrane-associated proteins FIXa and FX on the surface of activated platelets,[6,7] which promotes the enzymatic activation of FX by FIXa and thus restores blood clotting.

The binding properties of bsAbs are crucial for their function, as the propensity to form an interaction, the stability (half-life) of the interaction, and the equilibrium affinity, all influence the mechanism of action. For a binary interaction between two molecules, binding can be described in a straightforward manner by three biophysical parameters, namely, the association rate constant k_{on}, the dissociation
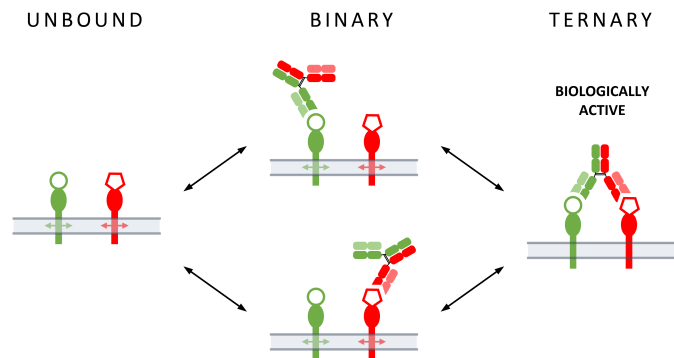
Figure 1. Binary- and ternary-binding modes of a bispecific antibody interacting with two targets on a cell surface.

rate constant k_{off}, and the dissociation constant in equilibrium $K_d = k_{off}/k_{on}$. For bispecific binders, the situation is more complex,[8,9] as one must consider two different binary interactions giving rise to a ternary interaction (Figure 1). Moreover, the ternary complex may be stabilized or destabilized by other cooperativity factors, such as the steric alignment of the three binders, conformational flexibility, or the local concentrations of molecular moieties participating in the interaction.[4,10–13]

The formation and decay of the ternary complex is governed by a dynamic interplay of all involved interactions, which is summarized by the term avidity. For example, the ternary complex gets disrupted when one arm releases its antigen. If the second arm detaches as well, the complex will dissociate completely, but the ternary complex will be reformed if the first arm swiftly rebinds its target. Thus, the stability of the ternary complex is determined by the association and dissociation kinetics of all possible (un)binding situations. Due to this interdependence of multiple parameters, separate measurements of binary-binding kinetics are not adequate to predict the behavior of the ternary complex.

Conventional methods to analyze molecular interactions are not well suited for the characterization of ternary complexes involving bsAbs.[8,14] Binding values derived from common surface plasmon resonance (SPR) measurements have been reported to deviate significantly from ELISA assays and biological activity.[15] This may be because SPR or similar sensors cannot discriminate whether a bsAb engages one or two targets on the sensor surface, since refractive index sensing detects the mere presence of analyte molecules on the sensor, but does not recognize how many bonds are established during an interaction.[8] Further, it is challenging to immobilize more than one antigen on the surface at well-defined stoichiometries when using conventional covalent immobilization strategies on dextran-modified surfaces. To circumvent this, SPR(-like) measurements of bsAbs are usually run as three-step assays,[16] where the bsAb is sandwiched between an immobilized first antigen (ligand) and the second antigen in solution (analyte). While this procedure can establish if the bsAb recognizes both targets in a qualitative manner, quantitative data interpretation is complicated because more than one analyte needs to be handled experimentally, and the observed signal is ill-defined because it represents the convolution of two or more

dissociation processes. The most critical limitation, however, is that a sandwich assay format does not reflect the situation of two antigens being presented to the bsAb on the same cell surface at the same time, which gives rise to avidity in the antibody's binding behavior. In the case of emicizumab, for example, this is crucial, as avidity is, in fact, the required binding mode on the natural platelet surface during FX activation,[17] and hence a prerequisite for biological activity.

Three requirements can be formulated for biophysical analytical methods to be impactful in the development of bsAb drugs, which target two antigens on the same cell. The first requirement is biological similarity. The antigens must be displayed next to each other on the sensor surface in a way that best emulates the conditions on a cell membrane regarding antigen mobility, accessibility, and control over antigen stoichiometry. The second requirement is full kinetic information. Kinetic rate constants must be analyzable for the affinity of individual binary interactions as well as for the avidity of the ternary complex, to be able to rationally engineer optimal-binding properties and to achieve the desired mechanism of action. Finally, high throughput is required. The workflow must be suitable to screen up to tens of thousands of interactions within a reasonable timeframe of several days to weeks. For comparison, 200 binders against each of the two targets of emicizumab were considered during its development, which amounts to 40,000 possible bispecific candidates, if all combinations were to be tested.

Here, we describe the development of an automated assay on a commercially available biosensor system that addresses these requirements, and we characterize binary- and ternary-binding properties of the bispecific therapeutic antibody emicizumab. For the immobilization of antigens on the sensor we devised and used a flexible, Y-shaped DNA nanostructure[18] that renders both targets accessible to binding by the solute bsAb. Using two-color fluorescence detection, we can follow the binding of emicizumab's individual paratopes to their respective targets FIX and FX in real-time. This is done separately for both targets, and for the cooperative engagement of both targets simultaneously, which allows us to dissect affinity and avidity-binding modes.

Results

The assay was developed on a commercial fluorescence biosensor system (heliX®), consisting of an automated instrument and chips with microfluidic channels featuring two sensor spots (Figure 2(a)). The sensor surface is functionalized by DNA-encoded addressing, whereby 'ligand strands' with the targets (ligands) of interest, FIX and FX, are automatically immobilized via hybridization to surface-tethered 'anchor' 48 deoxynucleotide single strands via complementary 'adapter' strands. Protein-DNA conjugates of FIX and FX were prepared before the sensing experiments using a commercially available amine-reactive coupling kit (see **Supplementary Figure S1 A, B**). The conjugates were incubated with adapter strands to self-assemble into Y-shaped DNA structures, as shown in Figure 2 (b,c) and **Supplementary Figure S1 C**.

The DNA Y-structure facilitates a flexible attachment of the two targets on the sensor surface and holds them in proximity
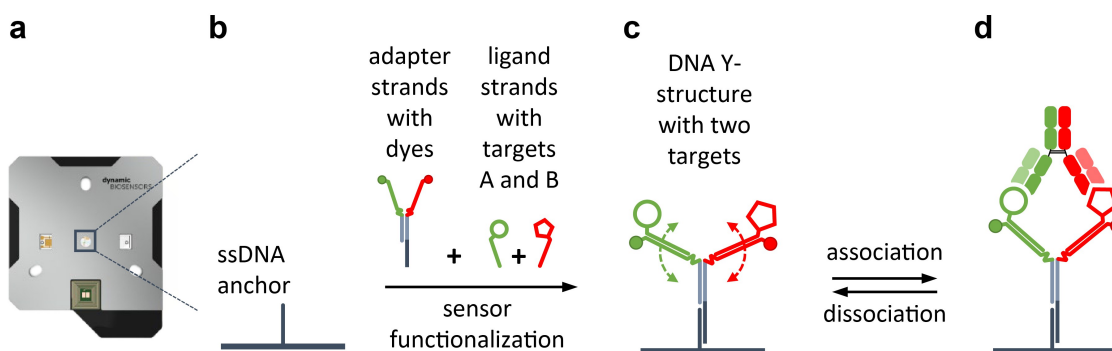
Figure 2. (a) heliX® biochip with a microfluidic channel featuring two detection spots; (b) single-stranded anchor oligodeoxynucleotides are covalently attached to the sensor's gold surface to enable further functionalization with DNA; the DNA Y-structure consists of two universal adapter strands that are modified with green and red dyes for fluorescence detection (full circles), and two ligand strands conjugated to the respective targets (FIX = open circle, FX = open pentagon); pre-formed Y-structures are immobilized through hybridization of their base to the 'anchor' strand on the sensor surface (c) Biosensor surface functionalized with DNA Y-structure, featuring two flexible arms for antigen-display at variable distances.; (d) Emicizumab bound to FIX and FX targets. Changes in the fluorescence of green and red dyes, which are in proximity to the individual targets, are measured to analyze the binding of antibody arms to FIX and FX, respectively.

for optimal binding. It is made up of a 96 bp stem branching into two 48 bp arms, at which ends the targets are attached. A single-stranded hinge region provides flexibility and rotational freedom of the arms. Based on arm and hinge lengths, the targets can move (diffuse) across an inter-target distance from 0 nm to approximately 40 nm. The flexible arm movement emulates the lateral mobility of targets on a cell membrane and permits the targets to adopt an optimal distance for binding to the two emicizumab antigen-binding fragments (Fabs) (Figure 2(c,d)). For detection, the Y-structure carries a green fluorophore on one arm, next to the first target (FIX), and a red fluorophore on the second arm, next to the second target (FX). Notably, the dyes are not attached to the analyte or ligand molecules, which remain label-free. Each dye is

a sensitive reporter of its molecular environment because its fluorescence intensity changes in response to the binding of analyte (bsAb) within the dye's reach, i.e., a few nanometers. This way, the association and dissociation of analyte can be observed for each target individually and simultaneously, which makes it possible to detect if the bsAb engages one target, the other target, or both targets at the same time.

Binary and ternary interactions of emicizumab with its targets were characterized for three different Y-structure configurations: FIX only, FX only, and FIX and FX simultaneously. The different configurations were prepared by mixing ligand strands featuring, or lacking, the respective targets during the Y-structure self-assembly step. Emicizumab was injected as solute analyte at six different
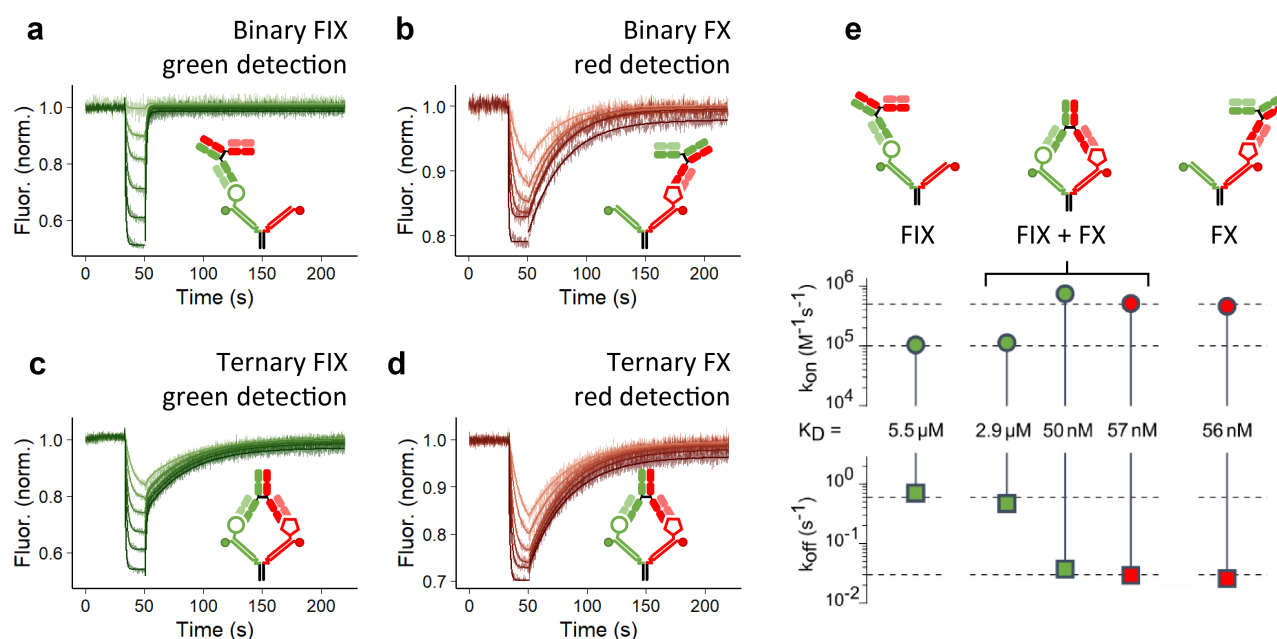

Figure 3. Real-time measurements of association and dissociation of Emicizumab to FIX and FX immobilized on a DNA Y-structure. The bsAb emicizumab was injected at concentrations of 0.0512, 0.128, 0.32, 0.8, 2, 5 μM. (a) Binary FIX – emicizumab interaction measured on a Y-structure modified only with FIX (no FX), signal detection in green. (b) Binary FX – Emicizumab interaction measured on a Y-structure modified only with FX (no FIX), signal detection in red. (c) and (d) Ternary interaction measured on a Y-structure modified with FIX and FX. Signals were measured simultaneously in green (C) and red (D). (e) Rate-scale plot of analyzed association (top) and dissociation (bottom) rate constants, together with the dissociation constant K_D (middle). Binary interactions (a, b) and the ternary FX interaction (D) were analyzed with single-exponential fit functions, the ternary interaction on the FIX arm (C) was analyzed with a bi-exponential fit function. Fit lines are drawn as smooth lines over measurement data, which were sampled at 200 ms.

concentrations from 0.05 to 5 μM and allowed to react with its targets (ligands) on the sensor surface for 15 s during the association phase. Dissociation was monitored for 180 s in constant buffer flow. Binding of emicizumab could be evidenced clearly for both targets by a transient quenching of fluorescence in the green (FIX) and red (FX) channels, respectively.

First, the kinetics of binary interactions were measured by loading either FIX or FX onto the Y-structure, while leaving the other arm unmodified. Sensorgrams are shown in Figure 3(a, b). The real-time signals could be fitted well globally with single-exponential functions, as expected for one-to-one interactions. Association and dissociation rates are summarized in the rate-scale plot in Figure 3(e) and Table 1. Emicizumab binds FIX and FX in a very dissimilar manner, clearly favoring FX. It associates 5 times faster and remains bound 20 times longer to FX than to FIX. Taken together, this results in a 100-fold higher affinity for FX (K_d = 56 nM) compared to FIX (K_d = 5.5 μM). These results confirm immunoassay data by Kitazawa et al., which were inconsistent with SPR data obtained by the same group.[15]

Ternary binding was investigated by loading the Y-structure with both targets. The detection of green and red fluorescence channels allowed us to follow the association and dissociation kinetics to FIX and FX individually and simultaneously (Figure 3(c,d)). For the strong interactant FX, the kinetics observed in the ternary experiment were practically identical to the binary experiment. For the weak interactant FIX, however, the outcome of the ternary and binary experiments differed substantially: ternary kinetics are not monophasic, but biphasic with two components resembling FX-like and FIX-like binding, respectively.

The finding that the ternary K_d was identical to the binary FX-K_d is an unusual result, so we performed control experiments using an antibody with two arms featuring equal affinities. The binary- and ternary-binding modes were analyzed for a monospecific, bivalent anti-digoxigenin monoclonal IgG interacting with a Y-structure that had been functionalized with digoxigenin (**Supplementary Figure S2** and **Supplementary Table S1**). In contrast to emicizumab, the anti-digoxigenin IgG indeed showed a pronounced avidity enhancement when both arms were engaged, namely, the avidity of the ternary-binding mode (K_d = 1 pM) was found to be 75 times stronger than the affinity of the binary mode (K_d = 75 pM), which confirms that the Y-structure assay detects avidity enhancement,

if there is any. Thus, we conclude the emicizumab result is not an artifact, but is related to the bsAb's specific properties, namely, the very different affinities of emicizumab's arms.

To examine the Y-structure assay format further, we addressed the question if the bsAb binds two targets on the same Y-structure (homo complex) or rather interlinks two adjacent Y-structures (hetero complex). We surmised that if interlinking occurs, it should depend on the average distance between Y-structures on the surface and would be more pronounced on high-density surfaces. Therefore, we performed measurements with four different Y-structure surface densities from 12.5% to 100% (**Supplementary Figure S3**). The observed kinetics were practically identical, irrespective of the Y-structure density used. This indicates that either (1) the bsAb preferentially binds to two targets on the same Y-structure (no interlinking of adjacent Y-structures) or (2) a bsAb that interlinks two Y-structures features the same binding properties as a bsAb that binds to a single Y-structure. Interlinking could in fact be observed in control experiments with the monospecific bivalent IgG binding to Y-structures that were modified with only one target (shown in **Supplementary Figure S2**). In spite of this, we assume that on Y-structures carrying two targets, the engagement of both targets on the same Y-structure is the dominant binding mode because it should be kinetically favored. The distance between two adjacent Y-structures is large compared to the proximity (high local concentration) of targets on the same Y-structure, and thus the formation of a ternary complex on the same Y-structure should be more likely.

To elucidate the origin of the biphasic kinetics observed for the ternary complex on the FIX arm further, we analyzed the relative contributions of FX-like and FIX-like binding for different emicizumab concentrations. As exemplified in Figure 4(a), the dissociation phase was fitted with a sum of two exponential functions. The amplitudes of the two exponential functions are analyzed in Figure 4(b). With increasing concentrations of injected emicizumab, the contribution of the fast, FIX-like process to the dissociation of the ternary complex increases, while the slow, FX-like process diminishes. This behavior pertains to the ternary complex, but is not observed when only one type of target is immobilized, where monophasic dissociations are observed, irrespective of the analyte concentration used (Figure 3(a,b)). Evidently, the dissociation behavior of the ternary complex depends on the concentration of emicizumab during the association phase.

Table 1. Kinetic rate constants (± fitting error).

|		Binary FIX	Ternary FIX	Ternary FX	Binary FX
Low stability interaction (FIX-like)	k_{on} (10^5 M^{-1}s^{-1})	1.27 ± 0.06	1.65 ± 0.25	–	–
	k_{off} (10^{-2} s^{-1})	70.2 ± 0.7	47.9 ± 2.6	–	–
	$t_{1/2}$ (s)	0.99 ± 0.01	1.45 ± 0.08	–	–
	K_D (μM)	5.53 ± 0.27	2.90 ± 0.47	–	–
	Amplitude	100%	variable	0%	0%
High stability interaction (FX-like)	k_{on} (10^5 M^{-1}s^{-1})	–	7.52 ± 0.49	5.16 ± 0.06	4.63 ± 0.08
	k_{off} (10^{-2} s^{-1})	–	3.73 ± 0.59	2.93 ± 0.01	2.58 ± 0.01
	$t_{1/2}$ (s)	–	19.1 ± 3.0	23.7 ± 0.1	26.9 ± 0.1
	K_D (nM)	–	49.6 ± 8.48	56.7 ± 0.68	55.8 ± 1.04
	Amplitude	0%	variable	100%	100%
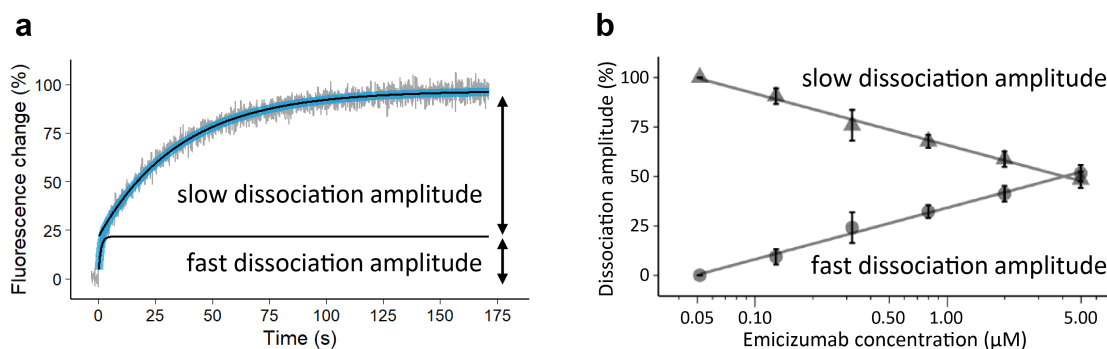
Figure 4. Analysis of ternary binding of emicizumab to FIX in the presence of FX at different concentrations. (a) Bi-exponential dissociation fit of the green signal on the FIX arm, exemplified by the measurement of 0.32 μM emicizumab. Curves of the individual single-exponential fit terms are shown as solid black lines, the compound curve (sum of two exponentials) is shown as a semitransparent thick blue line. The amplitudes of each exponential term are indicated as vertical arrows. (b) Analysis of the relative amplitudes of fast (FIX-like) and slow (FX-like) dissociations of emicizumab over different concentrations (n = 2).

Discussion

Our measurement of binary- and ternary-binding kinetics of the bsAb emicizumab yielded three important findings. First, the two binary interactions of the bsAbs to its two targets are markedly dissimilar, emicizumab binds FX 5x faster, 20x more stable, and overall 100x stronger than FIX. Second, ternary binding is distinctly different from binary binding and exhibits biphasic dissociation characteristics. Third, the extent of ternary binding that develops depends on the concentration of bsAb during the association phase. These results suggest the following interpretation, which is graphically summarized in Figure 5. As shown in Figure 5(a), formation of ternary complex occurs at low bsAb concentrations. In a first step, when emicizumab encounters the two targets presented by the Y-structure, it preferably binds to FX first, since the association rate is 5x higher than for FIX. In a second step, emicizumab's other arm engages FIX, which is presented within its reach by the Y-structure. Because the FX-bound emicizumab is already close to FIX, this hand-off happens quickly (compared to FX association), which is why a FX-like association rate is observed in the green signal for FIX, too. Of course, binary interactions between emicizumab with FIX or FX without formation of the ternary complex are also possible, as is the formation of the ternary complex through capture by the weaker interactant FIX, but these processes are much less likely to occur.

Decay of the ternary complex then follows. Once both targets are engaged, dynamic transitions occur between ternary and binary states. Due to the much weaker binding of FIX, however, it is likely that it is FIX, not FX, that is released and rebound by its Fab several or many times before the whole complex dissociates completely eventually. Hence, while interactions involving the weaker binder FIX are boosted by the presence of the strong binder FX, the FX interaction in turn is hardly affected by the presence of the weak interactant FIX, as it is too weak to significantly alter the kinetics of FX. Therefore, the kinetics observed for FX are similar for the binary and ternary cases. Compared with other bsAbs which often feature arms with similar binding kinetics, and where both arms confer
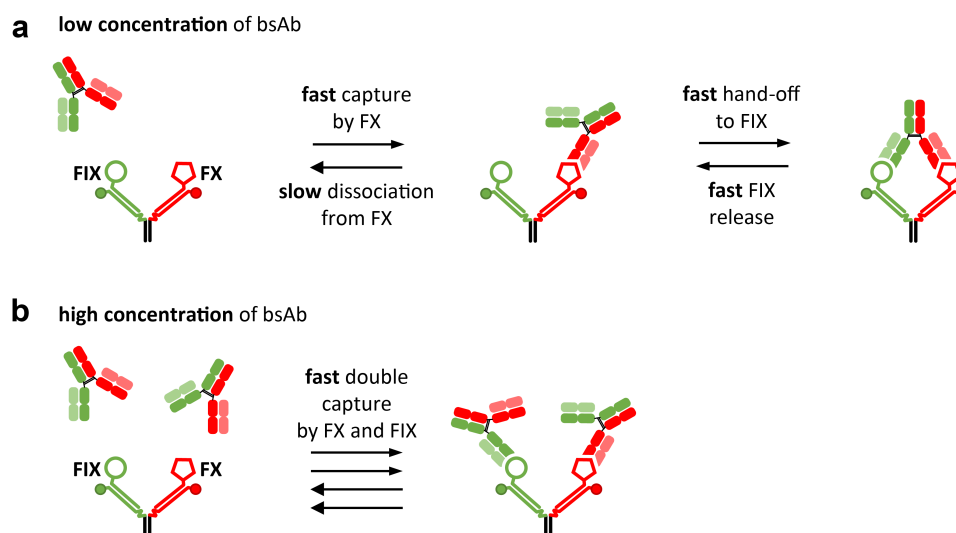

Figure 5. Schematic of emicizumab's dominant binding modes at low (a) and high (b) emicizumab concentrations. (A) At low analyte concentration, the faster association to FX captures the antibody and allows a rapid hand-off to FIX, resulting in a ternary complex. (B) At high analyte concentrations, the lower affinity FIX is rapidly binding an antibody as well, resulting in two binary interactions on one Y-structure. A combination of both (A) and (B) is observable as concentration-dependent bi-exponential dissociation curve.

stability to the ternary complex, emicizumab is quite special in that its Fabs feature markedly different affinities for their targets.

As shown in Figure 5(b), suppression of ternary complex formation occurs at high bsAb concentrations. At micro-molar concentrations of bsAb, the binding of bsAb from solution competes with the capture-and-hand-off mechanism that is facilitated by FX. This is expected to occur when the concentration of anti-FIX Fabs in solution exceeds the local concentration on the Y-structure, which has been determined to be in the 0.1–0.2 µM range. Therefore, double capture in binary-binding modes is favored when the bsAb concentration in solution is considerably higher than 0.1 µM. The finding that less ternary complex forms at higher analyte concentrations is reminiscent of the high dose "Hook" effect, which is a common interference in immunoassays.[19,20] Normally, during association one arm of the antibody binds to one target and then the second arm snaps onto the second target, forming the ternary complex. At high analyte concentrations, it becomes more likely that two antibodies simultaneously bind to one target pair, and thereby prevent the ternary complex formation.

Knowing these binding properties allows us to understand emicizumab's mode of action in vivo.[17] In blood plasma, FIX and FX are present at quite high concentrations of 90 and 135 nM, respectively.[7] Despite that Emicizumab is expected to interact frequently with both coagulation factors in solution, simulations show that only a negligible fraction of Emicizumab forms ternary complexes in plasma.[15] This is due to the fast dissociation from FIX, if its interaction is not stabilized by FX-mediated avidity on a surface. Only when FIX and FX are bound to activated platelets after an injury, a ternary complex with Emicizumab can be established.

Furthermore, the binding properties are related to the catalytic activation of FX. The catalytic rate constant of FX activation by the FIXa-emicizumab complex is 0.048 s^{-1},[15] corresponding to a catalytic half-time of 15 s. As a prerequisite for efficient activation, FIXa and FX must be held together by emicizumab long enough for the catalytic reaction to proceed. The experiments performed with surface-immobilized FIX/FX here show that the surface-mediated avidity effect is crucial in this respect, as it brings about a dissociation half-life of 20 s, which is long enough to facilitate a catalytic reaction. By contrast, in solution FIX dissociates from emicizumab within 1 s, which is too short to allow for catalytic activation. Therefore, FX does not get activated in plasma,[21] which would cause critical and potentially fatal side effects.

The characterized binding kinetics may also have predictive value for the in-vivo dose response. The efficacy curve should not just become saturated at high doses of emicizumab, but the drug's efficacy should be maximal at an optimal dose and decrease again for higher doses. This is a consequence of emicizumab's propensity to form binary complexes instead of ternary complexes with its target at high emicizumab concentrations. The optimal dose, which was roughly 0.1 µM for the Y-structure used here, depends on the effective surface concentration of FIXa and FX on the platelets. The more abundant FIXa and FX, the higher the dose for maximal efficacy can be, because the FX-to-FIXa handoff mechanism continues to work well. If FIXa and FX are depleted on the platelet, however, the optimal efficacy is expected at lower emicizumab dose.

In conclusion, the dual-color Y-structure assay was shown to provide valuable binding kinetics data for binary and ternary complexes of emicizumab and its targets FIX and FX. The workflow is well suited for the systematic screening of bispecific binders because it is based on a simple assay format and emulates the biologically relevant conditions on a cell surface. Both targets are co-immobilized at well-defined stoichiometry and local concentrations, and both targets are accessible to bind bispecific analytes. The assay is straightforward, as it does not require sequential injections like a sandwich assay, but uses only one analyte like in standard analyses for 1:1 interactions. Because the targets are preassembled onto the Y-structure, the workflow is economical in terms of sample consumption (400+ runs from one standard conjugation reaction) and can be automated easily. Screening of bispecific candidate molecules could be performed with detailed information about the interplay of kinetic rates, cooperativity, and binding times for each candidate. The assay format works over a wide affinity range, as could be demonstrated by the antibodies analyzed in this work, which featured K_ds in the µM, nM, and pM concentration ranges, and thus should be generally applicable. This allows targeted improvement of bispecific binders by affinity modulation of the individual binding moieties, as well as an optimization of their molecular structure and steric arrangement.

Materials and methods

Ligand conjugation

The targets FIX and FX were stably immobilized on the sensor surface via DNA connectors. To this end, proteins were coupled to single-stranded DNA ligand strands 1 and 2, respectively. 100 µg of FX (HFIX 1009, Enzyme Research Laboratories) and FIX (HFX 1010, Enzyme Research Laboratories) were conjugated via amine-coupling (NHS EDC chemistry) to 48mer DNA ligand strands 1 and 2, respectively (**Supplementary Figure S1 A**), using the kits HK-NHS-1 for FX and HK-NHS-4 for FIX (Dynamic Biosensors GmbH). The resulting DNA-protein conjugates were separated from remaining free protein, free DNA, and potential protein-DNA multimers by ion-exchange chromatography on a proFIRE instrument (Dynamic Biosensors) (**Supplementary Figure S1 B**). The final yield of DNA-protein conjugates was 25 µg for FX and 20 µg for FIX, which was sufficient to functionalize the sensor surface more than 500 and 400 times, respectively (approximately 50 ng of protein consumption per functionalization). Pure DNA-protein conjugates were stored in buffer PE40 (10 mM NaH_2PO_4/Na_2HPO_4, pH 7.4, 40 mM NaCl, 50 µM EDTA, 50 µM EGTA and 0.05% Tween20) and frozen at −80°C until use.

DNA Y-structure assembly

The Y-structure ligand was assembled using the assembly kit HK-YS-1B (Dynamic Biosensors). In short, a solution consisting of 100 nM of each adapter strand (with red and green dye, respectively) and 125 nM of each ligand strand (ligand 1-FX

and ligand 2-FIX) in PE40 buffer was incubated overnight at 4°C (**Supplementary Figure S1 C**). The assembled Y-structure was diluted at a ratio of 30:70 with c-Anchor 1 (DC-0, Dynamic Biosensors) to generate a 30% chip surface saturation. Lastly, the Y-structure mix was complemented with 100 nM of the oligo c-Anchor 2 (DC-0, Dynamic Biosensors) at a 1:1 ratio (v/v) directly before the functionalization for protection of the DNA anchor strands on the unused biochip reference spot. For control experiments with only one ligand on the surface, either ligand 1-FX or ligand 2-FIX were replaced by the respective empty ligand strands in the pre-hybridization (LFS-0, Dynamic Biosensors).

Binding kinetics measurements

Interaction between emicizumab (Hemlibra®; F. Hoffmann-La Roche AG, Basel, Switzerland) and FX and/or FIX was measured with the switchSENSE® technology on a heliX$^+$ instrument (Dynamic Biosensors) using standard adapter chips (ADP-48-2-0, Dynamic Biosensors) in static fluorescence proximity sensing (FPS) mode. The standard workflow for the measurement of kinetic rates was set up with the heliOS software v1.6.4 (Dynamic Biosensors). First, the chip surface was regenerated to obtain single-stranded DNA anchor strands on the electrode surface, which were then functionalized with the pre-hybridized Y-structure ligands. From kinetic measurements, emicizumab was diluted in running buffer (10 mM Tris, 140 mM NaCl, 50 μM EDTA, 50 μM EGTA, 0.05% Tween 20, 2.5 mM CaCl$_2$, pH 7.4) to the indicated concentrations, which were considerably higher than the femtomolar limit of detection of the instrument. Each association had a contact time of 15 s at a flow rate of 200 μl/min. The dissociation was recorded for 180 s, while running buffer was pumped over the surface at 500 μl/min. The heliX instrument allows selection of individual flow rate settings for association and dissociation phases, and so the flow rates were chosen as high as possible as a precautionary measure to avoid artifacts such as mass transport limitation and rebinding, while keeping the sample consumption to a minimum. Both association and dissociation were recorded at a sampling rate of 5 Hz. Before each injection of analyte, the surface was regenerated and functionalized with fresh Y-structure ligand.

Data analysis

Data from kinetic measurements were analyzed with the software heliOS (Dynamic Biosensors). The fluorescence signal was normalized to the baseline level and a buffer run was subtracted as blank reference. The kinetic rates k$_{on}$ and k$_{off}$ were obtained by fitting the data sets obtained with one target on the surface globally with mono-exponential fits of the association and dissociation phases. Data obtained with both targets on the surface were fitted globally with bi-exponential fits of the association and dissociation phases. The following fit functions were used:

Mono-exponential association and dissociation:

$$y = A \times \left[1 - exp\left\{ -\left(c \cdot k_{on} + k_{off} \right) \cdot t \right\} \right]$$
$$y = A \times exp\left\{ -k_{off} \cdot t \right\}$$

Bi-exponential association and dissociation:

$$y = A_{fast} \times \left[1 - exp\left\{ -\left(c \cdot k_{on,fast} + k_{off,slow} \right) \cdot t \right\} \right]$$
$$+ A_{slow} \times \left[1 - exp\left\{ -\left(c \cdot k_{on,slow} + k_{off,fast} \right) \cdot t \right\} \right]$$
$$y = A_{slow} \cdot exp\left\{ -k_{off,slow} \cdot t \right\} + A_{fast} \cdot exp\left\{ -k_{off,fast} \cdot t \right\}$$

Where y is the signal (proportional to fraction bound), A is the amplitude, c is the concentration of bsAb, k$_{on}$ is the association rate constant, k$_{off}$ is the dissociation rate constant. The affinity equilibrium dissociation constant is $K_d = k_{off}/k_{on}$, the avidity dissociation constant is $K_d = k_{off,slow}/k_{on}$. The half-life of the dissociation is $t_{1/2} = ln2/k_{off}$.

ORCID

Ulrich Rant (iD) http://orcid.org/0000-0002-6100-828X

References

1. Brinkmann U, Kontermann RE. Bispecific antibodies. Science (New York, NY). 2021;372:916–17. PMID: 34045345. doi:10.1126/science.abg1209.
2. White I, Tamot N, Doddareddy R, Ho J, Jiao Q, Harvilla PB, Yang T-Y, Geist B, Borrok MJ, Truppo MD, et al. Bifunctional molecules targeting SARS-CoV-2 spike and the polymeric Ig receptor display neutralization activity and mucosal enrichment. MAbs. 2021;13:1987180. PMID: 34693867. doi:10.1080/19420862.2021.1987180.
3. Kaplon H, Chenoweth A, Crescioli S, Reichert JM. Antibodies to watch in 2022. MAbs. 2022;14:2014296. PMID: 35030985. doi:10.1080/19420862.2021.2014296.
4. Mazor Y, Sachsenmeier KF, Yang C, Hansen A, Filderman J, Mulgrew K, Wu H, Dall'Acqua WF. Enhanced tumor-targeting selectivity by modulating bispecific antibody binding affinity and format valence. Sci Rep. 2017;7:40098. PMID: 28067257. doi:10.1038/srep40098.
5. Dovedi SJ, Elder MJ, Yang C, Sitnikova SI, Irving L, Hansen A, Hair J, Jones DC, Hasani S, Wang B, et al. Design and efficacy of a monovalent bispecific PD-1/CTLA4 antibody that enhances CTLA4 blockade on PD-1+ activated T cells. Cancer Discov. 2021;11:1100–17. PMID: 33419761. doi:10.1158/2159-8290.CD-20-1445.
6. Kitazawa T, Igawa T, Sampei Z, Muto A, Kojima T, Soeda T, Yoshihashi K, Okuyama-Nishida Y, Saito H, Tsunoda H, et al. A bispecific antibody to factors IXa and X restores factor VIII hemostatic activity in a hemophilia A model. Nat Med. 2012;18:1570–74. PMID: 23023498. doi:10.1038/nm.2942.
7. Yada K, Nogami K. Novel insights and new developments regarding coagulation revealed by studies of the anti-factor IXa (Activated Factor IX)/factor X bispecific antibody. Emicizumab

Arterioscler Thromb Vasc Biol. 2020;40:1148–54. PMID: 32237902. doi:10.1161/ATVBAHA.120.312919.

8. Drake A, Abdiche Y, Papalia G. 2018. Biophysical considerations for development of antibody-based therapeutics [Internet]. In Tabrizi M, Bornstein G, Klakamp S, editors. Development of antibody-based therapeutics. Singapore:Springer; cited 2022 Jul 13. p. 71–132.

9. Register AC, Tarighat SS, Lee HY. Bioassay development for bispecific antibodies-challenges and opportunities. Int J Mol Sci. 2021;22:5350. PMID: 34069573. doi:10.3390/ijms22105350.

10. Hampel PA, Strasser R, Fischer F, Rant U. Assembly and characterization of a slingshot DNA nanostructure for the analysis of bivalent and bispecific analytes with biosensors. Langmuir. 2018;34:14796–801. PMID: 30269507. doi:10.1021/acs.langmuir.8b02124.

11. Daub H, Traxler L, Ismajli F, Groitl B, Itzen A, Rant U. The trimer to monomer transition of tumor necrosis factor-alpha is a dynamic process that is significantly altered by therapeutic antibodies. Sci Rep. 2020;10:9265. PMID: 32518229. doi:10.1038/s41598-020-66123-5.

12. Jendroszek A, Kjaergaard M. Nanoscale spatial dependence of avidity in an IgG1 antibody. Sci Rep. 2021;11:12663. PMID: 34135438. doi:10.1038/s41598-021-92280-2.

13. Kast F, Schwill M, Stüber JC, Pfundstein S, Nagy-Davidescu G, Rodríguez JMM, Seehusen F, Richter CP, Honegger A, Hartmann KP, et al. Engineering an anti-HER2 biparatopic antibody with a multimodal mechanism of action. Nat Commun. 2021;12:3790. PMID: 34145240. doi:10.1038/s41467-021-23948-6.

14. Darling RJ, Brault P-A. Kinetic exclusion assay technology: characterization of molecular interactions. Assay Drug Dev Technol. 2004;2:647–57. PMID: 15674023. doi:10.1089/adt.2004.2.647.

15. Kitazawa T, Esaki K, Tachibana T, Ishii S, Soeda T, Muto A, Kawabe Y, Igawa T, Tsunoda H, Nogami K, et al. Factor VIIIa-mimetic cofactor activity of a bispecific antibody to factors IX/IXa and X/Xa, emicizumab, depends on its ability to bridge the antigens. Thromb Haemost. 2017;117:1348–57. PMID: 28451690. doi:10.1160/TH17-01-0030.

16. Mazor Y, Oganesyan V, Yang C, Hansen A, Wang J, Liu H, Sachsenmeier K, Carlson M, Gadre DV, Borrok MJ, et al. Improving target cell specificity using a novel monovalent bispecific IgG design. MAbs. 2015;7:377–89. PMID: 25621507. doi:10.1080/19420862.2015.1007816.

17. Lenting PJ, Denis CV, Christophe OD. Emicizumab, a bispecific antibody recognizing coagulation factors IX and X: how does it actually compare to factor VIII? Blood. 2017;130:2463–68. PMID: 29042366. doi:10.1182/blood-2017-08-801662.

18. Beike H, Daub H, Fjolla I, Langer A, Rant U, Strasser R . Method for detecting and/or characterizing the interaction between proteins and small molecules. US20200132678A1. Cited 2018 June 21 Application filed.

19. Schiettecatte J, Anckaert E, Smitz J. Interferences in Immunoassays [Internet]. IntechOpen. 2012; cited 2022 Jul 13. doi:10.5772/35797.

20. Ward G, Simpson A, Boscato L, Hickman PE. The investigation of interferences in immunoassay. Clin Biochem. 2017;50:1306–11. PMID: 28847718. doi:10.1016/j.clinbiochem.2017.08.015.

21. Shima M. Bispecific antibodies and advances in non-gene therapy options in hemophilia. Res Pract Thromb Haemost. 2020;4:446–54. PMID: 32548546. doi:10.1002/rth2.12337.